

The investigation of the mechanical properties of Mn doped BaSnO₃ nanoparticles

Iman Kazah¹ and R. Awad¹

¹ Physics Department, Faculty of Science, Beirut Arab University, Beirut, Lebanon
E-mail: ekazah93@gmail.com

Abstract. This study investigates the effect of Mn substitution on the structural and mechanical properties of nano BaSnO₃ using X-ray diffraction analysis (XRD), transmission electron microscopy (TEM), Scanning electron microscope (SEM) and Vickers microhardness. For this investigation, samples of type BaSn_{1-x}Mn_xO₃ with $0.04 \leq x \leq 0.4$ were prepared by co-precipitation method. XRD patterns indicate the formation of single phase cubic structure BaSnO₃ with space group (Pm3m) for $0 \leq x \leq 0.1$. BaMnO₂ hexagonal phase appears as impurity for $x > 0.1$. The crystallite size, increases as x increases. Vickers microhardness H_v was carried out at different applied loads varying between 0.98 N and 9.8 N at dwell time 40 seconds. The results show that H_v increases as the Mn-content increases, whereas it decreases as the applied load increase. The H_v results were analysed using Elastic Plastic Deformation and the Modified proportional specimen resistance models. The Vickers microhardness analysis indicates that Modified Proportional Specimen Resistance model is the most suitable one for describing the load independent microhardness region of the investigated samples.

1. Introduction

One of the interesting compounds, in materials science, for practical application as a sensor material for host gases [1,2], photocatalytic applications [3,4] and optical devices [5] is BaSnO₃. In the last few years, many preparation methods were reported to obtain nanoparticles of BaSnO₃ with cubic perovskite structure such as solid state reaction technique [6], sol gel method [7] and hydrothermal method [1,8]. One of the most suitable methods to prepare nanoparticles is the chemical co-precipitation method because of its simplicity and control of the crystalline size.

Balamurugan. et al reported the effect of transition elements such as Fe [9] and Mn [10] on the magnetic properties of BaSnO₃. They found that these samples exhibited a ferromagnetic behaviour at room temperature. Moreover, the mechanical properties of BaSnO₃ were studied by Maekawa et al. [11], where Vickers microhardness was found to be 5 Gpa. To our knowledge, there are no reports on the mechanical properties of BaSnO₃ doped by transition elements. Hence, the aim of this work is to study the effect of Mn doping on the mechanical properties of BaSnO₃ through Vickers microhardness investigation.

2. Experimental details

The nano-samples of nominal composition BaSn_{1-x}Mn_xO₃, with $0.04 \leq x \leq 0.4$, were prepared using co-precipitation method [12] where the starting materials were BaCl₂.2H₂O, SnCl₄.5H₂O and



MnCl₂·4H₂O. The nano-samples BaSn_{1-x}Mn_xO₃ were characterized by (XRD) analysis using Bruker D8 advanced power diffractometer with 20° < θ < 80° range and Cu-Kα radiation (λ = 1.54056 Å). The surface morphology was examined using Jeol transmission electron microscope JEM 100CX and Scanning electron microscope (SEM) ASC-200, respectively. Vickers microhardness measurements were performed using a digital microhardness tester H_v MHVD-1000IS by using equation (1) [13]

$$H_v = 1854.4 \times \frac{F}{d^2}, \quad (1)$$

where F is the applied load in Newton and d is the diagonal length of the indentation mark in μm.

3. Results and discussion

Figure 1 displays XRD patterns for BaSn_{1-x}Mn_xO₃ with 0 ≤ x ≤ 0.4. The major peaks indicate the formation of BaSnO₃ cubic perovskite with space group #221 (pm3m) up to x=0.1. For x > 0.1, BaMnO₂ peak was observed at 2θ = 31.2°. The lattice parameter a and the crystalline size D were estimated from Bragg's equation and Debye Scherrer's relation respectively [12], a and D are listed in table1. TEM and SEM for BaSnO₃ and BaSn_{0.9}Mn_{0.1}O₃ are presented in figure 2.

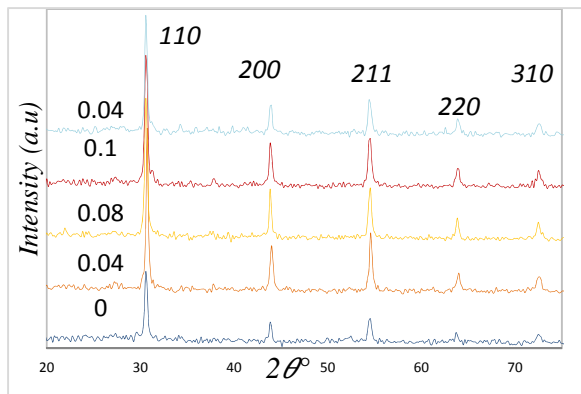


Figure 1. X-Ray diffraction patterns for BaSn_{1-x}Mn_xO₃ for x=0,0.04,0.08,0.1,0.4.

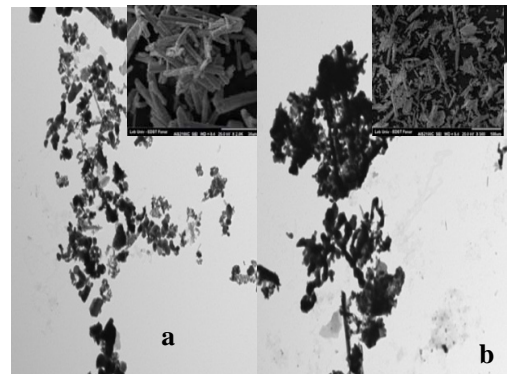


Figure 2. TEM and inserted SEM images for BaSn_{1-x}Mn_xO₃ samples for (a) x=0 and (b) 0.08.

The nano crystallites are of cuboidal shape with size ranging from 41-60 nm. The lattice parameter a fluctuates as x increases, where similar results were obtained by Ekaphan et al. [7] for BaSnO₃ doped by Fe. Figure 3 shows the variation of Vickers microhardness number H_v with the applied load F for BaSn_{1-x}Mn_xO₃ with x=0,0.04,0.08,0.1 and 0.4. H_v decreases non-linearly as the applied loads increase till about 3.00 N, and it tends to attain saturation till about 3.00 N. This behaviour can be explained on the basis of penetration depth of the indenter by Foerster et al. [14]. It is also noticed that H_v increases with the increase of x. This improvement can be attributed to the enhancement of resistance to crack propagation and due to the increase of cluster formation formed by Mn substitution.

The H_v results were analysed according to Elastic Plastic Deformation (EPD) and Modified Proportional Specimen Resistance (MPSR) models which are described by equations (2) and (3) respectively [15,16], the plots of the two models are represented in figures 4 a and b respectively. where A₁ is a constant, d₀ is the elastic component, α₁ corresponds to the minimum applied load to produce and indentation, α₂ and α₃ are related to the elastic and plastic properties of the material.

$$F = A_1(d + d_0)^2 \quad (2)$$

$$F = \alpha_1 + \alpha_2 d + \alpha_3 d^2, \quad (3)$$

Table 1. Lattice parameter (a), Crystallite size from XRD (DXRD), average particle size from TEM (DTEM) of BaSn_{1-x}Mn_xO₃ (x = 0,0.04,0.08,0.1 and 0.4) nanoparticles.

x	a (Å)	D _{XRD} (nm)	D _{TEM} (nm)
0	4.1118	50.0	60.0
0.04	4.1106	46.4	51.0
0.08	4.1148	44.2	48.0
0.1	4.1153	43.7	45.0
0.4	4.1176	42.4	41.0

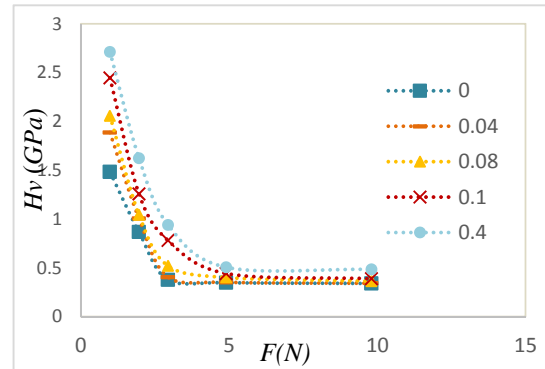


Figure 3. Variation of apparent H_v with $x=0.00, 0.04, 0.08, 0.1$ and 0.4 at different applied loads.

We notice from the figures that the experimental results are well fitted according to the 2 models. The fitting parameters for all models are listed in table 2. It is noticed from table 2 that the values of α_1 are positive for all samples, which indicates that the applied load is enough to create both the elastic and plastic deformations [15]. Moreover the values of d_0 are positive for all values of x which indicates that elastic deformation is present for all values of x . The True microhardness values obtained from EPD and MPSR approaches are calculated according to equations (4) and (5) respectively, and listed in table 2.

It is clear from table 2 that the values of H_{MPSR} are comparable with those obtained from experimental results. Whereas, it is noticed that EPD model displays much lower values than the experimental values H_v . Thus, the MPSR Model is the best fitted model for BaSn_{1-x}Mn_xO₃ samples.

$$H_{EPD} = 1854.4 \times \frac{F}{(d_0+d^2)} \tag{4}$$

$$H_{MPSR} = 1854.4 \times \frac{\alpha_1+\alpha_2d+\alpha_3d^2}{d^2} \tag{5}$$

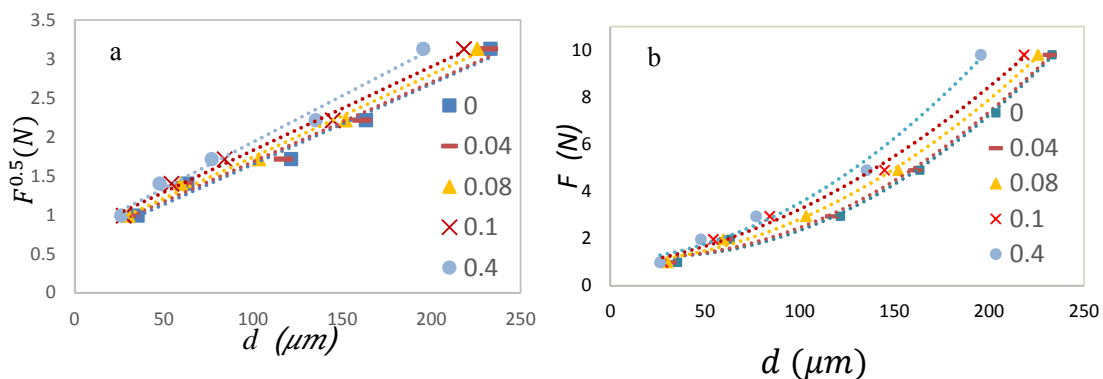


Figure 4. a. \sqrt{F} against d according to EPD model, b. F against d according to MPSR model.

Table2. Microhardness analysis results for different models and parameters for BaSn_{1-x}Mn_xO₃ samples with x= 0.00, 0.04, 0.08, 0.1, and 0.4; variation of Vickers microhardness values with respect to different applied models from experimental values calculated at $t = 40$ s.

x	EPD model		MPSR model			Vickers microhardness values		
	A_1 ($\frac{N}{\mu m^2}$)	d_0 (μm)	α_1 (N)	α_2 ($\frac{N}{\mu m}$)	α_3 ($\frac{N}{\mu m^2}$)	Hv experimental	Hv (EPD)	Hv (MPSR)
0.0	0.00011	68.77670	0.00004	0.0291	0.0002	0.3555	0.1864	0.3632
0.4	0.00010	73.00980	0.00002	0.0330	0.0002	0.3668	0.1833	0.3953
0.8	0.00011	70.41509	0.00002	0.0343	0.0002	0.4286	0.2019	0.4273
0.1	0.00012	72.63889	0.00003	0.0361	0.0001	0.5373	0.2143	0.5106
0.4	0.00013	70.73684	0.00002	0.0398	0.0002	0.6442	0.2617	0.6037

4. Conclusion

BaSn_{1-x}Mn_xO₃ where $0.00 < x < 0.4$ were successfully prepared using co-precipitation method. XRD results indicated that the substitution of Mn to BaSnO₃ did not affect the cubic crystal structure but slightly increased the crystallite size. TEM and SEM images assure the increase of grain size of the particles and showed the Mn clusters that appear at high doping. The Vickers microhardness values increased as x increased. By analyzing Vickers microhardness according to different models, it was noticed that H_v results obeyed the Modified Proportional Specimen Resistance model.

References

- [1] Maekawa T, Kurosaki K and Yamanaka S 2006 *J. Alloys Compd.* **416** 214–17
- [2] Deepa A S, Vidya S, Manu P C, Solomon S, John A and Thomas J K 2010 *J. Alloys Compd.* **509** 1830–35
- [3] Köferstein R, Jäger L, Zenkner M and Ebbinghaus S G 2009 *J. Euro. Ceram. Soc.* **29** 2317–24.
- [4] Borse P H, Joshi UA, Ji SM, Jang JS, Lee J S, Jeong E D and Kim H G 2007 *Appl. Phys. Lett.* **90** 034103–11.
- [5] Mizoguchi H, Woodward P M, Park C H and Keszler D A 2004 *J. Am Chem Soc* **126** 9796–9800.
- [6] Fu-an Guo, Guoqiang Li and Weifeng Zhang 2010 *International Journal of Photoenergy* doi:210.1155/2010/105878.
- [7] Ekaphan Swatsitang, Attaphol Karaphun, Sumalin Phokha and Thanin Putjuso 2016 *J Sol-Gel Sci Technol* **77** 78–84.
- [8] Lu W and Schmidt H 2005 *J. Euro. Ceram. Soc.* **25** 919–925.
- [9] Balamurugan K, Kumar H N, Chelvane J A and Santhosh P N 2008 *J. Alloys Compd* **472** 9–12.
- [10] Balamurugan K, Kumar H N, Ramachandran B, Ramachandra Rao M S, Chelvane A J and Santhosh P N 2009 *Sol. Stat. Commun.* **149**: 884–87.
- [11] Maekawa T, Kurosaki K and Yamanaka S 2006 *J. Alloys Compd.* **416** 214–17.
- [12] Rahal H T, Awad R, Abdel-Gaber A M and EL-Said Bakeer D 2016 *Journal of Nanomaterials* ID 7460323.
- [13] Leenders A, Ullrich M and Freyhardt H C 1997 *Phys. C* **279** 173.
- [14] Foerster C E, Lima E, Rodrigues Jr P, Serbena F C, Lepienski C M, Cantao M P, Jurelo A R and Obradors X 2008 *Braz. J. Phys.* **38** 341.
- [15] Awad R, Abou Aly AI, Kamal M and Anas M 2011 *J. Supercond Nov Magn* **24** 1947–1956
- [16] Rahal H T, Awad R, Abdel Gaber A M and Roumie M 2016 *J. Supercond Nov Magn* DOI 10.1007/s10948-016-3654-4